Chapter 5
Modal Parameters Estimation of an Offshore Wind Turbine Using Measured Acceleration Signals from the Drive Train

M. El-Kafafy, L. Colanero, N. Gioia, C. Devriendt, P. Guillaume, and J. Helsen

Abstract Offshore Wind Turbine (OWT) is complex structure that consists of different parts (e.g. foundation, tower, drivetrain, blades, ...). The last decade there is a continuous trend towards larger machines with the goal of cost reduction. Modal behavior is an important design aspect. For tackling NVH issues and validating complex simulation models it is of high interest to continuously track the vibration levels and the evolution of the modal parameters (resonance frequencies, damping ratios, mode shapes) of the fundamental modes of the turbine. Wind turbines are multi-physical machines with significant interaction between their subcomponents. This paper will exploit this and present the possibility of identifying and tracking consistently the structural vibration modes of the drivetrain of the instrumented offshore wind turbine by using signals (e.g. acceleration responses) measured on the drivetrain system. The experimental data has been obtained during a measurement campaign on an offshore wind turbine in the Belgian North Sea where the OWT was in standstill condition. The drivetrain, more specifically the gearbox, is instrumented with a dedicated measurement set-up consisting of 17 sensor channels with the aim to continuously track the vibration modes. The consistency of modal estimates made at consequent 10-min intervals is validated, and the dominant drivetrain modal behavior is identified.

Keywords Modal parameters • Offshore wind turbine • Drivetrain • Tower modes • Mode tracking

5.1 Introduction

There is a trend to increase the power produced by each individual turbine in order to reduce the cost of wind energy by the so-called upscaling trend. Bigger wind turbines have the advantage that they can harvest wind at higher altitudes, resulting in bigger wind speeds and allow the turbine to be equipped with bigger blades. Moreover, it is assumed that by decreasing the number of machines per Mega-watt the operations and maintenance costs of the wind park will decrease. Bigger wind turbines and corresponding blades impose higher loads on the wind turbine components, amongst others on the drive train. Moreover, these loads cannot be assumed to be quasi-static as in most industrial applications. Wind turbine loading includes aerodynamic loads at variable wind speeds, gravitational loads and corresponding bending moments, inertial loads due to acceleration, centrifugal and gyroscopic effects, operational loads such as generator torque and loads induced by certain control actions like blade pitching, starting up, emergency braking or yawing [1–4]. These dynamic loads are significantly influencing the fatigue life of the wind turbine structural components. In addition to the tower and blades also the drivetrain has several structural components for which the design is fatigue driven, such as for example the torque arms of the gearbox. In addition to turbine reliability also noise and vibration (N&V) behavior is becoming increasingly important for onshore turbines [5]. Since aerodynamic noise is decreasing by means of improved blade designs, the problem

M. El-Kafafy (✉)
Vrije Universiteit Brussel (VUB), Pleinlaan 2, B-1050 Brussel, Belgium

Helwan University, Cairo, Egypt
e-mail: melkafaf@vub.ac.be

L. Colanero • P. Guillaume • J. Helsen
Vrije Universiteit Brussel (VUB), Pleinlaan 2, B-1050 Brussel, Belgium

N. Gioia
Université Libre De Bruxelles, Brussles, Belgium

C. Devriendt
Vrije Universiteit Brussel (VUB), Pleinlaan 2, B-1050 Brussel, Belgium

OWI-lab, Brussel, Belgium

C. Niezrecki (ed.), *Structural Health Monitoring & Damage Detection, Volume 7*, Conference Proceedings of the Society for Experimental Mechanics Series, DOI 10.1007/978-3-319-54109-9_5

is shifting towards drivetrain tonalities. Accurate insights in the dynamic behavior are necessary to avoid these tonalities. This is because bigger turbines imply that the resonance frequencies of the drivetrain are decreasing towards the excitations coming from the wind turbine rotor and gears of the gearbox [4]. Therefore, the flexibility of the structural components of the drivetrain is becoming increasingly of influence on the dynamic design of the drivetrain [6]. Accurate knowledge about the resonance behavior of the drivetrain is as such essential for improved design both for fatigue and reliability as for noise. If resonances are coinciding with harmonic excitation frequencies, there is potential for increased fatigue life consumption and tonal excitation. Operational modal analysis (OMA) has proven its' use in aerospace and automotive and is increasingly used nowadays in the wind energy domain. There are different frequency ranges of interest for the wind turbine. The lower frequency range contains the more global modes of the wind turbine, such as the blade modes, tower modes and general drivetrain modes. For the drivetrain, the higher frequency ranges contain more localized modes of the gearbox and generator.

This paper discusses a preliminary study for characterizing the challenges for the use of OMA for characterizing the dynamic behavior of the wind turbine drivetrain and by extension the other main components of the turbine. In this study, we investigate both frequency ranges and show the potential for OMA techniques to characterize the eigenfrequencies value, damping and mode shape for these resonances. We want to take the initial step towards the full dynamic characterization of the wind turbine by means of accelerometers mounted on the drivetrain. Since there is the chance with OMA techniques that harmonics can be misinterpreted as resonances, we want to avoid these conditions. Therefore, the turbine is investigated while it is not producing energy. In this case, harmonics do not dominate the frequency spectrum and modal estimation can be done in a reliable way.

5.2 Data Acquisition

A long-term measurement campaign with duration of 6 months was performed on an offshore wind turbine. Instrumentation was limited to the drivetrain. In total 17 accelerometer channels were acquired. 14 channels were originating from accelerometers on the gearbox. This consisted of four tri-axial sensors and two uni-axial sensors. One tri-axial accelerometer was placed on the generator. All accelerometers used were ICP accelerometers and a sensitivity of 100 mV/g. Three accelerometers had a high sensitive frequency range between 2 and 5000 Hz, whereas the other sensors were tailored for a range between 0.5 and 5080 Hz. It can therefore be stated that the measurement set-up was tailored towards the higher frequency range identification. In addition to detailed accelerometer measurements, the speed of the wind turbine rotor is measured by means of an encoder at the low speed shaft with 128 pulses per revolution. All data is sampled at 5120 Hz. In total 160 min of data is used in the analysis done in this paper (16 datasets of 10 min each).

5.3 Operational Modal Analysis and Modal Parameters Tracking Approach

This paper investigates the turbine modal behavior while it is not producing energy. This specific operating condition will have an impact on the modal behavior observed in the drivetrain, since the teeth can be out of contact during these conditions; whereas this is necessarily the case for nominal power production [7]. Moreover, the damping properties of the wind turbine will change according to the operating conditions [8]. This study will first focus on the low frequency bandwidth to characterize the global wind turbine modes. These consist of the modes of the main turbine components such as the blades and tower. As will be shown the turbine is a multi-physical system with high interaction between the different subcomponents. Therefore, not only the drivetrain modes, but also the blade and tower resonance frequencies are present in the acceleration signals measured on the wind turbine drivetrain. This study will not go into detail on the tracking of these modes. They are used as a means to validate the validity of the measurements performed and to get confidence in the results of the OMA techniques for the estimation of the modal parameters.

For the higher frequency modes, a manual tracking approach validates the consistency of the OMA technique. Modal parameter estimations are performed for 16 consecutive time blocks of 10 min each. The eigenfrequencies and damping values of five main resonances modes are tracked for the consecutive time blocks. Peak selection is performed manually. This is done in order to show the repeatability of the analysis and to underpin the applicability of this technique for characterizing drivetrain modal behavior.

For the modal parameter estimation, the polyreference least squares complex exponential (pLSCE) estimator [9–11] was used to extract the modal parameters from the processed measured signals. The frequency-domain data, which is the input to the pLSCE estimator, is generated using the Correlogram approach [12]. So, for each data block the auto and cross correlation functions are calculated using some signals as references. Then, the spectrum for each data block is calculated by applying

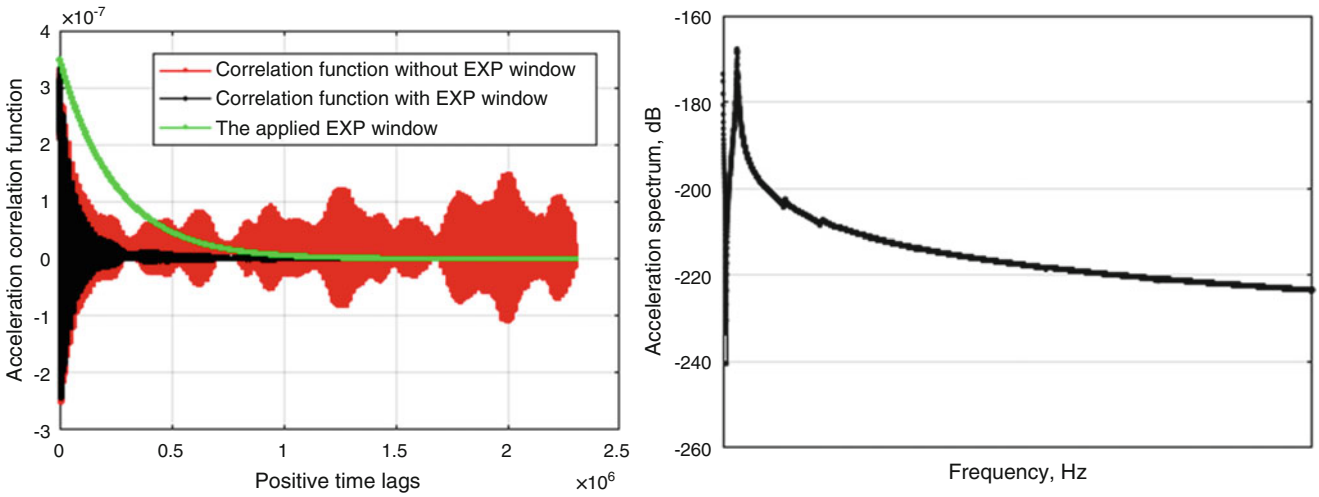

Fig. 5.1 Typical correlation function (*left*) and the corresponding spectrum (*right*) [the frequency axis is made hidden for confidentiality reason]

the FFT on the calculated auto and cross correlation functions. Figure 5.1 shows one typical correlation function and the corresponding calculated spectrum. An exponential window was applied to the correlation function before calculating the FFT to decease the leakage and noise effects. In the following, a brief description of the pLSCE estimator will be given, and the tracking steps will be summarized.

For operational modal analysis (OMA) applications, the pLSCE starts with the power spectrum of the measured outputs. The half power spectrum is defined as following in the form of a frequency-domain modal model assuming that the unmeasured inputs are white noise in the frequency band of interest:

$$S_{yy}^{+}(\omega_k) = \sum_{i=1}^{N_m} \frac{\Psi_r L_r^T}{j\omega_k - \lambda_r} + \frac{\Psi_r^* L_r^{*T}}{j\omega_k - \lambda_r^*} \in \mathbb{C}^{N_o \times N_{ref}} \tag{5.1}$$

where $\boldsymbol{S_{yy}^{+}} \in \mathbb{C}^{N_o \times N_{ref}}$ a matrix contains the positive (half) auto and cross power spectrum with $\boldsymbol{N_o}$ number of measured outputs and $\boldsymbol{N_{ref}}$ number of signals taken as references, $\boldsymbol{N_m}$ is the number of the identified modes, $\boldsymbol{\omega_k}$ is the circular frequency in r/s at frequency line $\boldsymbol{k}$, $\boldsymbol{\Psi_r} \in \mathbb{C}^{N_o \times 1}$ is the $\boldsymbol{r^{th}}$ mode shape, $\boldsymbol{L_r} \in \mathbb{C}^{N_{ref} \times 1}$ is the $\boldsymbol{r^{th}}$ operational reference factors vector, and $\boldsymbol{\lambda_r}$ is the pole of the $\boldsymbol{r^{th}}$ mode. The inverse Laplace transform of $\boldsymbol{S_{yy}^{+}(\omega_k)}$ gives the time-domain equivalent modal model that can be given as following:

$$h(kT_s) = \sum_{r=1}^{N_m} \psi_r z_r^k L_r + \psi_r^* z_r^{*k} L_r^* \tag{5.2}$$

with $z_r^k = e^{-\lambda_r k T_s}$ for the kth time sample ($k = 0, 1, 2, \cdots, N_s - 1$) and N_s is the number of time samples. Equation (5.2) is the time-domain version of the modal model (5.1) in which the "impulse" response function is decomposed as a sum of decaying sinusoids. The pLSCE estimator fits $h(kT_s)$ by means of a matrix polynomial model in a linear least-squares sense. Then, from the matrix coefficients of this polynomial the poles and the reference factors are calculated. In a second step, with having the calculated poles and the operational reference factors the mode shapes can be calculated from Eq. (5.1) as an explicit function of the poles, the operational reference factors, and the measured $S_{yy}^{+}(\omega_k)$ by solving a linear least-squares problem.

The different steps that are done to manually track the modal parameters of the different modes in the frequency-band of interest can be summarized as following:

1. Read and load the time-domain data (16 measured acceleration records of 10 min each)
2. Correlogram approach is applied to calculate the auto/cross power spectra matrix
   a. Specific signals are selected to be taken as reference signals
   b. The auto and cross correlation functions are calculated between the outputs signals and the selected reference signals
   c. Exponential window applied to the correlation functions to decrease the noise and leakage effects
   d. Fast Fourier Transform is applied to the correlation function to calculate the spectra matrix
3. The pLSCE estimator is applied to the spectra matrix with wide range of model orders

4. The stabilization diagram is constructed
5. The different physical modes are manually selected from the stabilization diagram
6. Damping is corrected to remove the exponential window effects
7. Tracking frequencies, damping values and mode shapes

This tracking approach will be applied to 16 datasets of 10 min collected during the measurements campaign on the drivetrain of the instrumented offshore wind turbine while the wind turbine was in stand still condition. It should be mentioned here that for the modes selection from the stabilization diagrams over the different datasets, efforts have been made to select as much as possible the same mode at the same model order.

5.4 Results and Discussions

As it was mentioned in the introduction and Sect. 5.3, the main objective of this measurement campaign was to do dynamic characterization of the drivetrain of the instrumented OWT. Since a detailed knowledge about the specifics of the drivetrain itself is not available, it is suggested to first validate the quality of the measurements and the reliability of the tracking approach (i.e. data preprocessing, modal parameter estimation step, etc). To do so, a short-term tracking of the modal parameters of the modes of the turbine's tower and blades will be done over the different 16 datasets measured from the drivetrain, and the results from this analysis will be compared to the ones obtained using signals acquired from sensors mounted on the tower of the same turbine. These modes are detected in the low frequency range. After validating the measurements quality and the reliability of the modes tracking approach, analysis in a bit higher frequency band will be done with the aim to track some physical vibration modes of the drivetrain itself. In the analysis of both the high and low frequency-bands, the frequency values will not be shown for confidentiality reason.

5.4.1 Low Frequency-Band Analysis

According to the results obtained using signals acquired from some accelerometers mounted on the tower of the instrumented turbine, It can be concluded that the physical vibration modes of the tower and the foundation system of the instrumented OWT are dominantly present in the low frequency band and they are labeled as following:

- First for-aft bending tower mode (FA1)
- First side-side bending tower mode (SS1)
- Mode with a second for-aft bending mode tower component (FA2)
- Mode with a second side-side bending mode tower and nacelle component (SS2N)
- Mode with a second for-aft bending mode tower and nacelle component (FA2N)

In addition to the tower modes, some other modes related to the blades and the drivetrain can be also detected in this low frequency band. Those modes are the first drivetrain torsional mode (DTT1), the first blade asymmetric flapwise pitch (B1AFP) mode, the 1st blade asymmetric flapwise yaw (B1AFY) mode, the 1st blade collective flap (B1CF) mode, and the 1st blade asymmetric edgewise yaw (B1AEY) mode.

The tracking approach explained in Sect. 5.3 is applied to the 16 datasets of 10 min each acquired from the accelerometers mounted on the drivetrain of the instrumented OWT. Figure 5.2 shows an example for the stabilization diagram constructed by the pLSCE estimator in the low frequency-band. The shown stabilization diagram indicates that there are several modes located in that band. The dominant peak corresponds to the first for-aft (FA1) and first side-side (SS1) bending modes of the tower, which are characterized by a lot of motion at the nacelle level according to the visualization of their mode shapes. The most dominant modes of the tower, blades, and drivetrain are estimated and tracked over the 16 datasets measured from the drivetrain sensors. The standard deviation values of the estimated resonance frequencies values of the tower and blades modes are presented in Tables 5.1 and 5.2. From Table 5.1, one can see that the most dominant tower modes are successfully detected except the third mode, i.e. FA2. Based on the mode shapes results of the tower modes estimated using sensors mounted on the tower itself, it was noted that the FA2 mode is mostly dominated by tower motion and not a motion at the nacelle level. This can explain why this mode is not well-detected using signals measured from the drivetrain system. It can be seen from Table 5.1 that the frequency of the third mode (i.e. SS2N) is estimated with a higher uncertainty in comparison with the other tower modes. This can be explained by the fact that it was noted from the tower mode shapes that the motion at the nacelle level is less for the SS2N mode in comparison with the FA1, SS1, and FA2N modes. In general, the low standard deviation values shown in Tables 5.1 and 5.2 confirms that the tower and the blades modes are successfully and consistently estimated over the different 16 datasets.

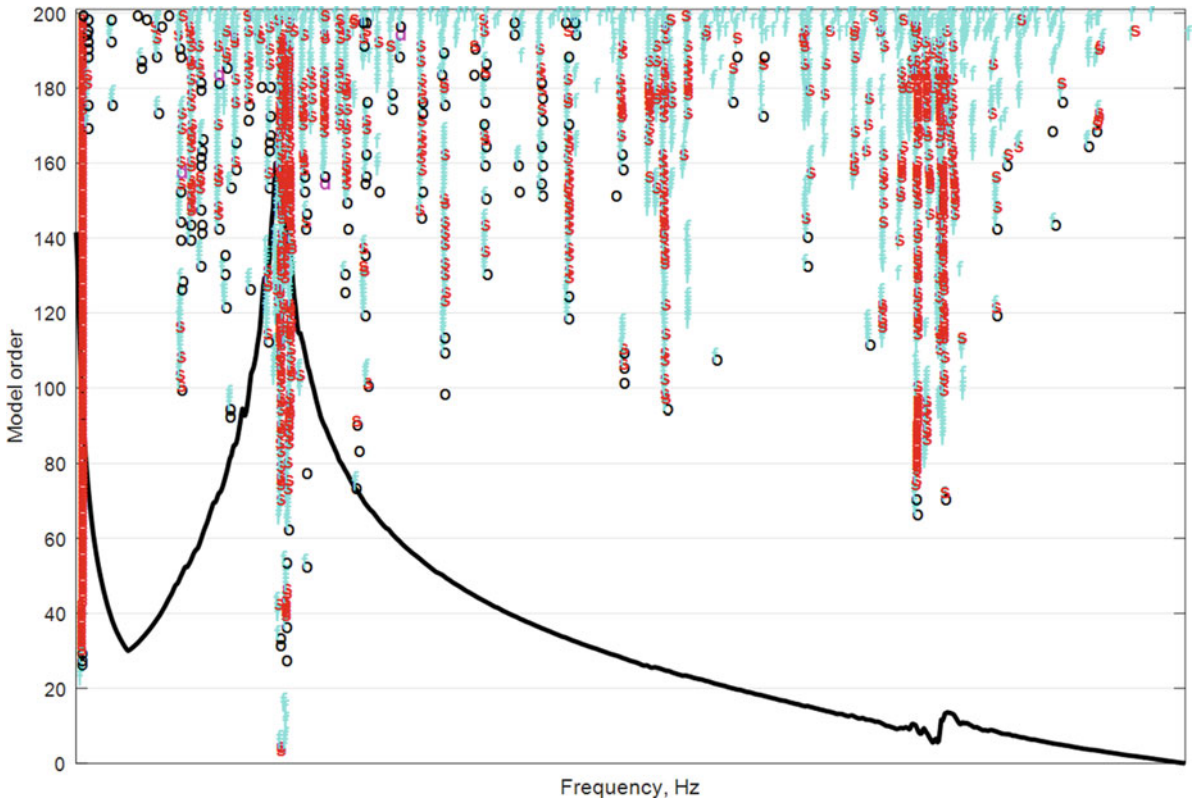

Fig. 5.2 Low frequency band analysis: typical stabilization diagram constructed by the pLSCE estimator

Table 5.1 Results of the short-term tracking of the low frequency-band modes (Tower modes)

Mode	Std freq. Hz
FA1	0.007
SS1	0.003
SS2N	0.022
FA2N	0.006

Table 5.2 Results of the short-term tracking of the low frequency-band modes (Blade and drivetrain modes)

Mode	Std freq. Hz
B1AEY	0.021
B1AFP	0.031
B1AFY	0.015
B1CF	0.005
DTT1	0.028

A comparison between the tower modes frequencies estimated using the drivetrain signals and the signals measured on the tower of the same turbine is shown in Fig. 5.3. From this figure it can be seen that the mean values agree very well and the confidence bounds are overlapping. The higher standard deviation on the SS1 and FA2N modes estimated using tower signals is really due to the fact that these estimates are calculated based on 2016 datasets representing a monitoring period of 2 weeks. Therefore, this higher standard deviation is mainly driven by the environmental variations rather than the quality of the estimation itself. It is also noted that the frequency values obtained for the blades modes agree very well with the ones estimated when processing the signals measured from sensors mounted on the tower. In Fig. 5.4, the mode shapes of the drivetrain system at the FA1 and SS1 resonance frequencies are shown. From these mode shapes, one can see that the movement of the drivetrain system resembles the tower movement where it goes in the for-aft direction (x-dir.) at the tower FA1 frequency and in the side-side direction (Y-dir.) at the tower SS1 frequency. Therefore, the consistency of the obtained results the ones obtained from signals measured directly on the tower of the same turbine confirms the correctness of the measurements, especially considering that the sensors that have been used on the drivetrain are aimed towards higher frequency region for dynamic analysis of the drivetrain.

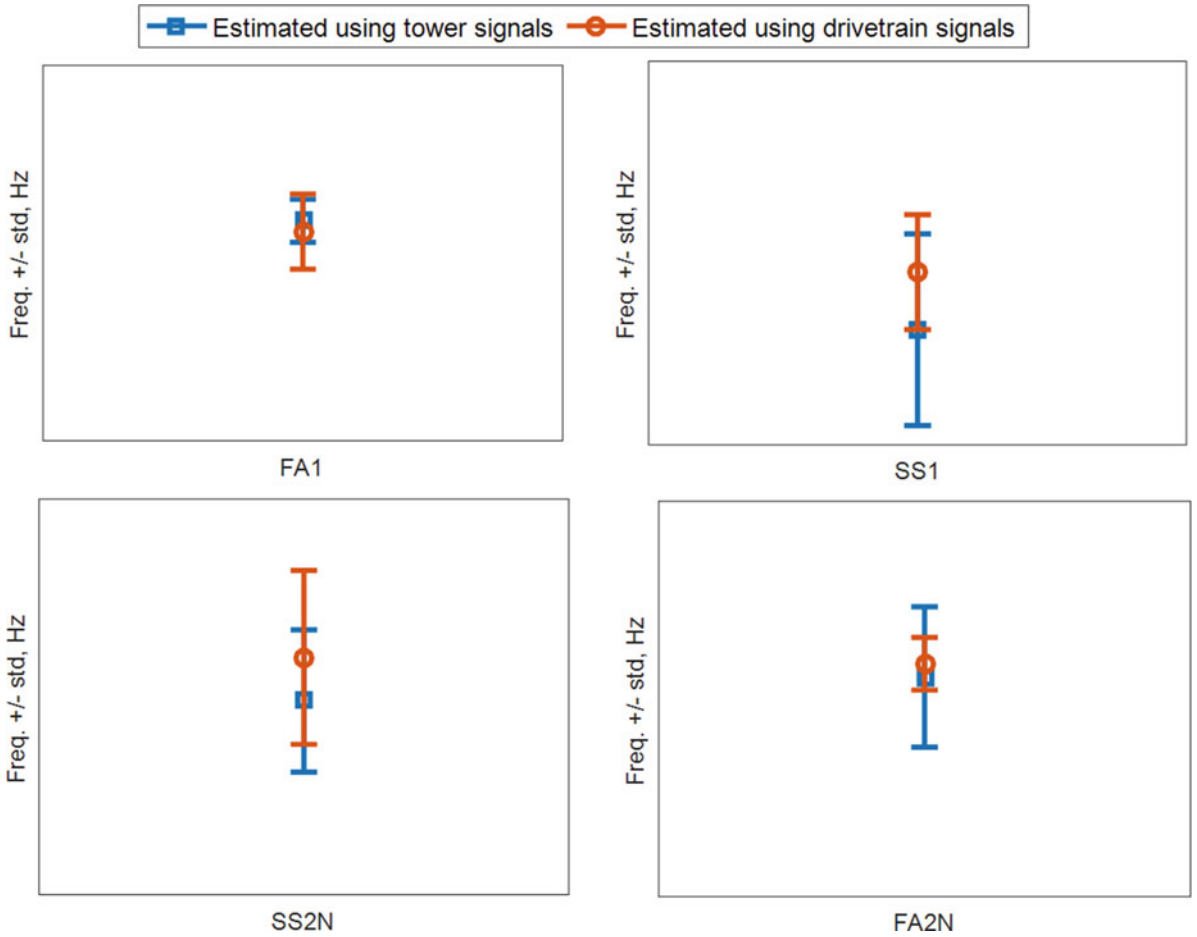

Fig. 5.3 Low frequency-band analysis: Comparison between the estimated resonance frequencies values of the tower global modes using the drivetrain signals and tower signals

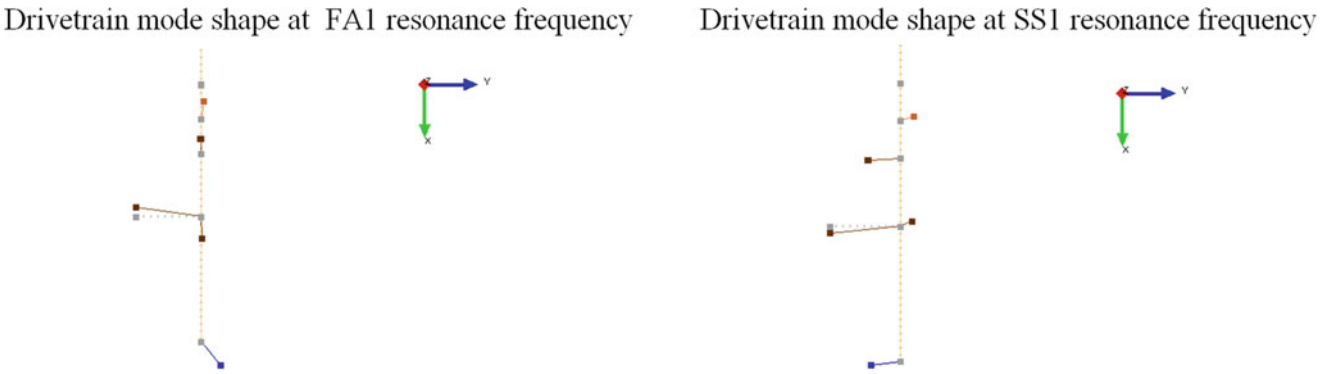

Fig. 5.4 The drivetrain mode shapes corresponded to the tower FA1 frequency (*left*) and at the tower SS1 frequency (*right*) (*Y*: Side-Side direction *X*: For-Aft direction *Grey dots*: undeformed model)

5.4.2 High Frequency-Band Analysis

Using the 16 datasets of the acceleration signals measured from the drivetrain system and by means of the tracking approach presented in Sect. 5.3 the first results of the short-term tracking of some modes of the drivetrain will be presented in this section. The analysis frequency band will be extended a bit in comparison to Sect. 5.4.1 to include some higher frequency modes, which are thought to be mainly the drivetrain modes. Figure 5.5 shows one stabilization diagram constructed by the pLSCE estimator in the frequency band of interest. The blue arrows in the stabilization diagram refer to the five modes

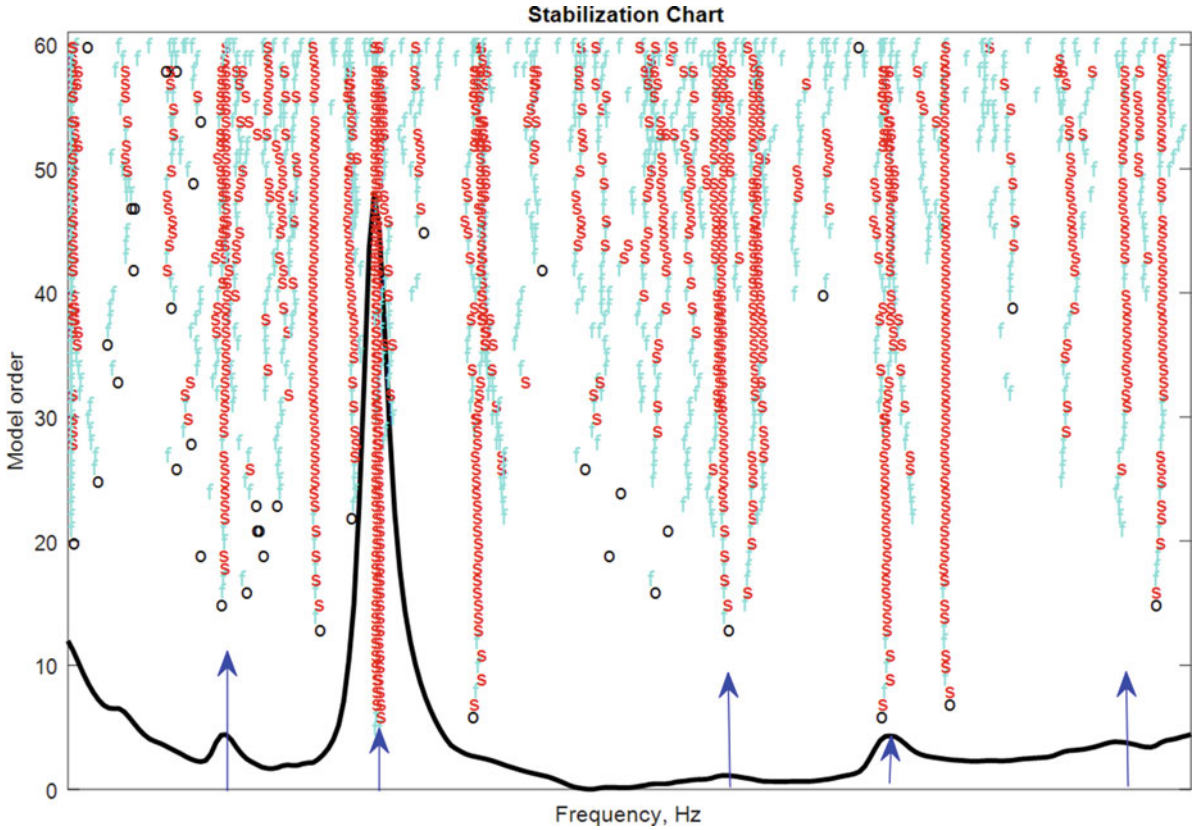

Fig. 5.5 Higher frequency-band analysis: stabilization chart constructed by the pLSCE estimator [the frequency axis is made hidden for confidentiality reason]

that will be tracked over the 16 datasets. These modes are selected after doing some preliminary analysis like, checking the correlation of the mode shapes between the different modes in the band (i.e. MAC criterion), checking the rate of the existence of the mode in all the 16 datasets, and the coincidence of the mode to a peak in the spectrum. The result of the short-term tracking in terms of the resonance frequencies and damping ratios of the five modes is shown in Fig. 5.6. This figure illustrates one box and whisker plot per frequency and damping value of each tracked mode. The results in this figure show that for all the modes the resonance frequency values show high level of consistency over the different data blocks. In terms of damping value, the second, third, fourth, and fifth modes show low scatter in comparison to the first mode. This level of the consistency of the results over the different 16 processed datasets shows the repeatability of the analysis and underpins the applicability of the measurements and the modal estimation approach for the characterizing drivetrain model behavior.

5.5 Conclusions

The modal behavior of an OWT is investigated while the OWT was in stand still condition. The investigation is done by performing a short-term manual tracking of the modal parameters of the different components of the turbine, e.g. tower, blades, and drivetrain system. The signals used to estimate the modal parameters are 17 acceleration signals acquired from tri-axial and uni-axial accelerometers mounted on the drivetrain system (i.e. gearbox and generator) of the turbine. In the low frequency-band analysis, the consistency of the obtained results with the ones obtained when using signals measured from sensors mounted on the turbine's tower confirms the validity of the measurements performed and give confidence in the OMA technique used for the estimation of the modal parameters. The analysis done in the high frequency-band is an initial step towards the full dynamic characterization of the modal behavior of the drivetrain system. The results there show the repeatability of the analysis and confirm the applicability of the used technique for characterizing the drivetrain modal behavior considering stand still condition. Further investigations for the modal behavior of the drivetrain will be continued, and an automatic tracking approach could be done.

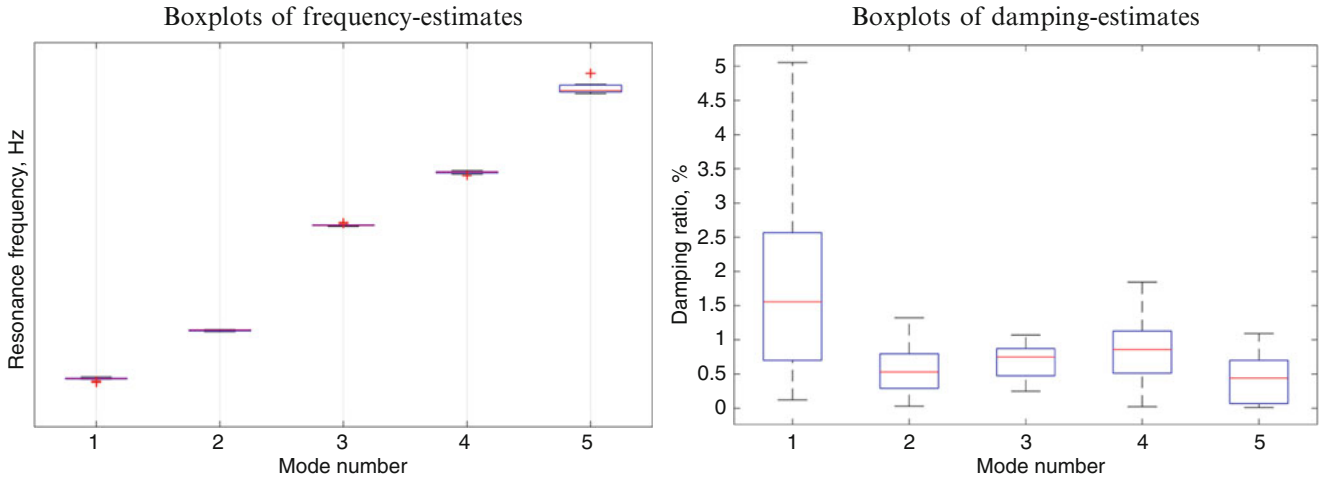

Fig. 5.6 Boxplots of the frequencies (*left*) and damping values (*right*) of the five dominant modes in the high-frequency band. On each box, the central mark is the median, the edges of the box are the 25th and 75th percentiles, the whiskers extend to the most extreme values that were not considered as outliers and the outliers are plotted individually using the '+' symbol

Acknowledgements The authors would like to acknowledge the VLAIO SBO HYMOP and Proteus Project, as well as the farm owner and OEM for facilitating the measurement campaign.

References

1. Veers, S.P.: Three-dimensional wind simulation. Technical report SAND88e 0152.UC-261, Sandia (1988)
2. Mann, J.: Wind field simulation. Prob Eng Mech. **13**(4), 269e82 (1998)
3. Peeters J. Simulation of dynamic drive train loads in a wind turbine. PhD thesis, Division PMA, Department of Mechanical Engineering, Belgium: Katholieke Universiteit Leuven, Leuven (Heverlee) (2006). Available online: http://hdl.handle.net/1979/344
4. Peeters, J., Vandepitte, D., Sas, P.: Analysis of internal drive train dynamics in a wind turbine. Wind Energy J. **9**, 141e61 (2006)
5. Goris, S., Ribbentrop, A., et al.: A validated virtual prototyping approach for avoiding wind turbine tonality. In: 5th International Conference on Wind Turbine Noise Denver (2013)
6. Helsen J. The dynamics of high power density gearboxes with special focus on the wind turbine application. PhD thesis, Division PMA, Department of Mechanical Engineering, Belgium: Katholieke Universiteit Leuven, Leuven (Heverlee) (2012)
7. Vanhollebeke, F., Peeters, P., Helsen, J., Di Lorenzo, E., Manzato, S., Peeters, J., Vandepitte, D., Desmet, W.: Large scale validation of a flexible multibody wind turbine gearbox model. J. Comput. Nonlinear Dyn. **10**(4), 041006 (2015)
8. Weijtjens W., Shirzadeh R., De Sitter G., Devriendt C. Classifying resonant frequencies and damping values of an offshore wind turbine on a monopole foundation for different operational conditions. In: Proceedings of EWEA, Copenhagen (2014)
9. Brown, D.L., Allemang, R.J., Zimmerman, R., Mergeay, M.: Parameter estimation techniques for modal analysis. SAE Transactions, paper No. 790221, vol. 1979, pp. 828–846 (1979)
10. Vold, H., Numerically robust frequency domain modal parameter estimation, Sound and Vibration, 24(1), 38–40.
11. Vold, H., Kundrat, J., Rocklin, G., Russel, R.: A multi-input modal estimation algorithm for mini-computers. SAE Trans. **91**(1), 815–821 (1982)
12. Bendat, J., Piersol, A.: Random Data: Analysis and meaurment procedures. Wiley, New York (1971)